

Structure of Extremely Nanosized and Confined In-O Species in Ordered Porous Materials

J.M. Ramallo-López,¹ M. Rentería,² E.E. Miro,³ F.G. Requejo,^{1,4} and A. Traverse²

¹Departamento de Física, FCE, Universidad Nacional de La Plata, C.C.N. 67, 1900 La Plata, Argentina

²LURE, Université Paris-Sud, Bât. 209 A, B.P. 34, 91898 Orsay Cedex, France

³INCAPE (FIQ, UNL, CONICET), Santiago del Estero 2829, 3000 Santa Fe, Argentina

⁴Lawrence Berkeley National Laboratory, One Cyclotron Road-Mailstop 66-200, Berkeley CA 94720, USA

(dated: March 22, 2022)

Perturbed-angular correlation, x-ray absorption, and small-angle x-ray scattering spectroscopies were suitably combined to elucidate the local structure of highly diluted and dispersed InO_x species confined in porous of ZSM-5 zeolite. This novel approach allows us to determine the structure of extremely nanosized In-O species exchanged inside the 10-atom ring channel of the zeolite, and to quantify the amount of In_2O_3 crystallites deposited onto the external zeolite surface.

The study of structural, magnetic and electronic properties of nanostructured, subnanostructured and, in the other extreme, highly diluted monocationic species in solids deserves increasing attention not only from a fundamental point of view but also for their technological applications [1]. In one extreme, highly-dispersed metallic exchanged-atoms in an infinite variety of compounds present, e.g., very important catalytic properties [2], which are not clearly correlated with the active species responsible for them since their physical entities are often unknown. The design of new catalysts with improved activity, selectivity and stability requires the complete knowledge of the local environment of the active centers and its correlation with the desired reaction. The complete characterization of this kind of structures is at present a challenging problem not only in catalysis but also in many fields of physics.

An additional difficulty is the confinement of the diluted species inside porous materials. In general, experimental techniques based on energetic probes that strongly interact with the materials, may destroy them. On the other side, low energetic probes are unuseful since they have to pass through the walls around the "hidden" locations of the confined clusters or atoms and their kinetic energy is attenuated.

The importance of the extended X-ray absorption fine structure (EXAFS) spectroscopy to study structural properties in crystalline solids [2], nanoclusters [3] and highly dispersed ionic species in catalysis [4] has been long acknowledged. EXAFS constitutes a powerful "atom selective" technique to extract direct information about type, number and distances of neighbors of the absorber atom [5, 6]. However, in EXAFS analysis, if more than one species has the same type of bonds (same element and similar bond-lengths), the information from each one would be almost impossible to extract directly, unless some additional information is known.

The perturbed-angular-correlation (PAC) technique requires a suitable probe-atom (native or foreign) to be in the system under study, being in this sense also "atom se-

lective". PAC enables the precise determination – at the probe site – of the electric-field gradient tensor (EFG), which is extremely sensitive to the anisotropy of the electronic density near the nucleus, which in turn reflects the probe-neighboring coordination. PAC has been intensively applied to many fields in science during the past two decades with success [7] and, very recently, to the development of accurate *ab initio* calculations of the EFG at diluted impurity sites in crystalline solids [8]. However, structural information is not easily obtained if we are dealing with highly dispersed, disordered, and coexistent multiple-species.

In this letter, we will show that the combination of gamma- and X-ray-based techniques like PAC, EXAFS, and small-angle X-ray scattering (SAXS) can be a novel and powerful experimental tool that can be applied to the emerging field of structure determination of extremely nanosized and confined species, like In-species at exchange sites in ZSM-5 zeolites.

The crystalline zeolite framework, an aluminum-silicate structure crossed by channels and cavities, is a challenging laboratory to study the exchange and deposition of confined particles in internal surfaces. It has been shown [9] that In exchanges at Al acid sites of the zeolite and, due to its specific surface, 90 % of these sites are inside the channels. In/ZSM-5 is known as a promising catalyst in one of the major topics in environmental catalysis, the selective catalytic reduction (SCR) of nitric oxides by hydrocarbons [9, 10]. The nature of the active sites for SCR with methane (SCRM) in In/zeolite catalyst has been extensively studied but only little qualitative information about them has been obtained [11]. Ogura et al. [9] showed that the active site in In/ZSM-5 for the SCRM are intrapore In species, and suggested that they are $(\text{InO})^+$ oxoions coordinated at the Z exchange sites of the zeolite. Very recently, Schmidt et al. [12] reported an exhaustive spectroscopic study of the structure of In-species (not necessarily active) using several preparation methods to synthesize In/ZSM-5. Since they did not succeed to obtain a sample with an iso-

TABLE I: Fitted hyperfine parameters values that characterize the interactions observed in the PAC spectrum of Fig. 1.

Site	f (%)	ν_Q (Mrad/s)	η (%)	ν_Q (Mrad/s)
I ₁	41 (5)	19.0 (2)	0.72 (1)	1.4 (2)
I ₂	13 (2)	25.0 (1)	0.14 (2)	1.7 (4)
I ₃	46 (2)	32.2 (5)	0.33 (3)	9.1 (1.0)

lated active species they have not attempted to extract a particular In-O distance among several oxygen neighbors to verify the existence of the In-oxo site. In a previous work we studied in detail the several In species that can arise using different preparation methods and activation treatments, leading to highly active catalysts [10]. By means of the PAC technique we characterized this system and quantified the amount of In active sites. However, little information about the structure of this species could be obtained because of the high distribution of its hyperfine frequency and the lack of accurate EFG calculations. In this work we have therefore selected the preparation route that yields to the largest amount of the active species and with the rest of In atoms forming bulk In_2O_3 at the external surface of the zeolite.

$\text{NH}_4\text{-ZSM-5}$ with a Si/Al ratio of 26.4 obtained as in Ref. 10 was used as starting material. Indium was incorporated to the zeolite by the conventional wet impregnation method, stirring an aqueous solution of InCl_3 (added in an amount as to obtain a sample with 4 wt% of In) and $\text{NH}_4\text{-ZSM-5}$ at 80°C until all water was evaporated, followed by drying in a stove at 120°C for 12 h. After this, the solid was pretreated in a dried oxygen atmosphere heating up to 500°C at $5^\circ\text{C}/\text{min}$, and holding the final temperature for 12 h. Afterwards, the sample was calcined for 2 h in oxygen at 750°C . In order to perform the PAC experiments the probe ^{111}In was introduced by adding traces of $^{111}\text{InCl}_3$ to the non-radioactive InCl_3 solution. ^{111}In decays by electron-capture to excited states of ^{111}Cd , which reaches the ground state mainly through a γ -cascade with an intermediate nuclear state of quadrupole moment Q that interacts with the EFG existing at the probe site. This EFG, which perturbs the γ -angular correlation, can be determined by measuring the time modulation of the γ -coincidence rate. A four BaF_2 -detector fast-fast coincidence system in a coplanar 90° arrangement was used to measure the γ -coincidence spectra, which are combined to form the anisotropy ratio $R(t)$. This $R(t)$ can be expressed as the sum of cosine functions of three interaction frequencies from which the strength, V_{zz} , and symmetry, $\eta = (V_{xx} - V_{yy})/V_{zz}$, of the diagonalized and traceless EFG tensor can be determined. If the probes are located at different sites, their relative concentration f_i can also be determined model independently. A detailed description of the technique can be found elsewhere [13]. Figure 1 shows the PAC spectrum for the $\text{In}(^{111}\text{In})/\text{ZSM-5}$ sam-

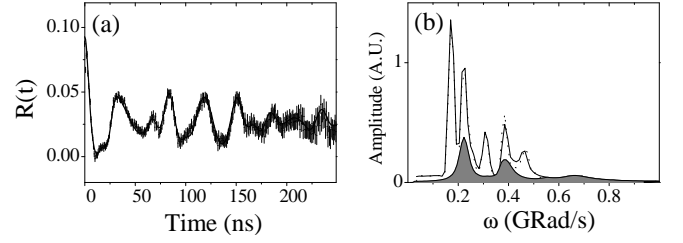


FIG. 1: (a) PAC spectrum of $\text{In}(^{111}\text{In})/\text{ZSM-5}$ measured at 500°C in air. Solid line is the least-squares fit of theoretical $R(t)$ function to the data. (b) Fourier transforms of the $R(t)$ spectra (dashed line), of the $R(t)$ fit (solid line), and the contribution of I_3 (shaded curve).

ple taken at 500°C in air, and its corresponding Fourier transform. It should be noted that no after-effects due to the electron-capture decay of ^{111}In are present, as expected at this temperature [14]. In Table I, the fitted hyperfine parameters f_i , $\nu_Q = eQV_{zz}/4\pi\hbar$, and η (that accounts for a Lorentzian EFG distribution around a mean ν_Q value originated from a distribution of very similar neighborhoods of the probe for a certain site) are shown. The three hyperfine interactions indicate that In occupies three different sites. The first two (I_1 and I_2) correspond to ^{111}In in the two inequivalent sites of In_2O_3 present in the expected 3:1 population ratio [14], and the third one (I_3) with a concentration of 46% corresponds to the catalytically active species, since it has been shown that In_2O_3 is not active for the reaction of interest [10]. The low values of I_1 and I_2 agree well with the fact that crystallites of very small dimension are really a minority in the sample. The slight deviation from axial symmetry of site D has been already reported for crystalline In_2O_3 [15].

The In K-edge (27940 eV) X-ray absorption coefficients were measured at the D42 beam line (XAS13 station) of the DCI synchrotron at LURE. The spectra were recorded with 4 eV steps at room temperature in air using a two-crystals Ge400 monochromator and Kr gas in the ionization chambers. The EXAFS data were extracted from the measured absorption spectra by standard methods [16]. The spectra were Fourier-transformed in order to obtain the radial distribution functions around In atoms in the samples. This function gives a view of the atomic distribution around the absorber, with peaks at distances where neighboring shells are located. The height of the peaks is related to the type and coordination number (CN) of neighbors. The study of small particles by EXAFS could lead to average coordination numbers (ACN) smaller than those expected for the bulk because of the contribution of atoms in the surface. The structural and thermal disorder, and a distribution of slightly different surroundings for a certain site (accounted for by the Debye-Waller factor, σ^2) could also reduce the height of the peaks. Figure 2 shows the K-edge EXAFS

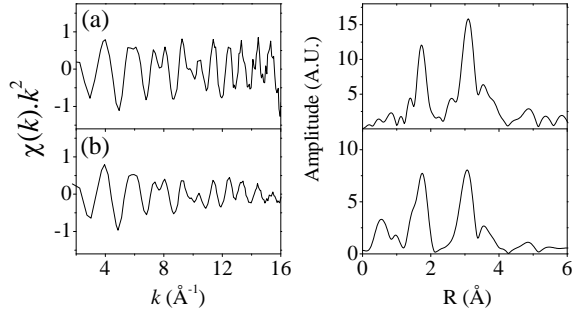


FIG. 2: In K-edge EXAFS spectra (right) and their Fourier transforms (left) of (a) In_2O_3 ; (b) In/ZSM5 catalyst.

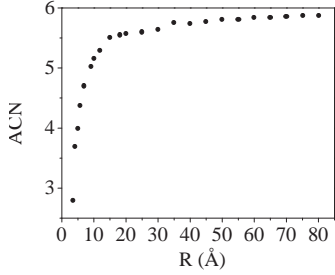


FIG. 3: A CN of In at the symmetric site in In_2O_3 .

spectra of In_2O_3 and In/ZSM5 as well as their Fourier transforms. At first sight, both spectra differ only in the smaller amplitude of the second one. As there is a mixture of indium species in the catalyst – In_2O_3 and In-oxo active species – and both of them have In-O bonds with overlapping bond-length, it is not possible to fit directly the EXAFS spectra to obtain a deconvoluted information of one of them. In contrast, if doing so we would obtain an average of the In CN of both species weighted by the relative abundance of each species in the catalyst. Even though it should be possible to propose a two-shells fitting of the spectrum with modified CN's, this procedure will not lead to a unique solution. At this point, the relative fractions of each species obtained from ^{111}In -PAC measurements in a model-independent way could be used to isolate the active species by subtracting the spectrum of In_2O_3 weighted with its relative fraction, a method similar to the difference technique used to isolate a minor component from the major components in an EXAFS spectrum [5]. Nevertheless, there is one thing that must be considered, i.e., the size of the In_2O_3 crystallites. The parameter of the symmetric site D observed in the PAC experiments suggested that small crystallites of In_2O_3 could be present. Figure 3 shows the A CN of In at the symmetric site of neutral spherical particles of In_2O_3 for different particle sizes, obtained averaging the CN of each In atom in the particle. As can be seen, the A CN grows rapidly for small particles and approaches the CN of the bulk (CN=6) for radii greater than ca. 20

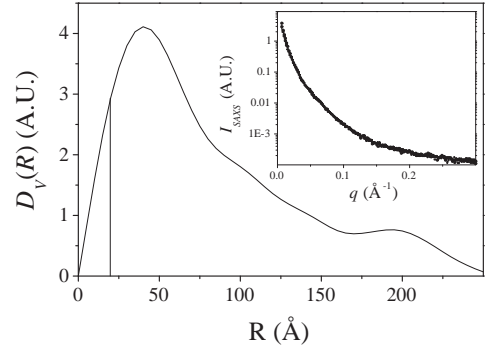


FIG. 4: Cluster volume distribution of In_2O_3 crystallites in In/ZSM5. The vertical line corresponds to $R=20$ Å. The SAXS profile of the In_2O_3 particles is shown in the inset.

TABLE II: EXAFS results of the In K-edge difference spectrum of Fig. 5. E_0 is the inner-potential correction.[5]

Shells	CN	Bond-Length (Å)	σ^2 (Å ²)	E_0 (eV)
In-O	0.9(2)	2.10(1)	0.003(8)	2.2(3)
In-O	2.1(2)	2.20(1)	0.011(8)	2.2(3)
In-Al	1.1(2)	2.59(1)	0.046(8)	4.7(3)

Å. This implies that, if the In_2O_3 particles present in our sample are very small (with radii of the order of 5 to 10 Å), the subtraction of the In_2O_3 bulk spectrum to the In/ZSM5 one would lead to an overestimation of the In CN and hence to an underestimation of the CN of the active species. On the contrary, if the sesquioxide particles are bigger than 20 Å in radius, their A CN would be larger than 5.5 and it could be correct, in a first approximation, to subtract the In_2O_3 bulk spectrum to obtain that of the other species present in the catalyst.

Hence, the SAXS technique was used to determine the volume distribution of indium oxide particles in the In/ZSM5 catalysts. SAXS experiments were performed at the SAS beam line [17] at the National Synchrotron Light Laboratory (LNLS-Campinas, Brazil). The cluster volume distribution function $D_V(R)$ [18] of the In-O_x particles is shown in Fig. 4. This function was determined from the SAXS intensity profile (Fig. 4, inset) using the GNOM package [19]. This profile was obtained as usual [20] by subtracting the ZSM5 normalized SAXS spectrum to that of the In/ZSM5 catalysts to get rid of the scattering contribution coming from the porous ZSM5 support. Figure 4 shows that there is a broad distribution of In_2O_3 particle sizes in the catalysts and there is a maximum of $D_V(R)$ at $R=50$ Å with a long tail to larger radii. Although there are small particles with $R < 20$ Å, its relative fraction is very small. Partial integration of the curve shows that 93% of the volume corresponds to particles with radius bigger than 20 Å. For particles bigger than 20 Å in radius, the average coordination number is close to that of the bulk and the dif-

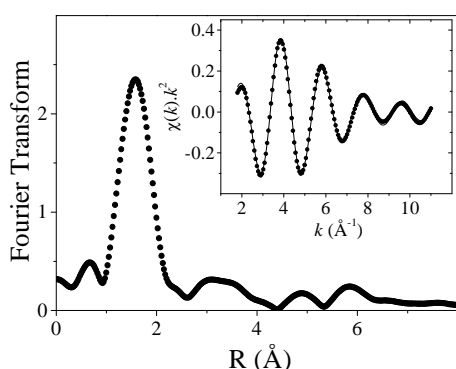


FIG. 5: Amplitude of the Fourier transform of the difference spectrum corresponding to In species at exchange sites (circles). In the inset, back-transform of the peak in the range 0.9-2.6 (dots) and its EXAFS fit (solid line).

ference can be included within the experimental error for the CN (ca. 10%). Under these circumstances, it is valid to subtract the EXAFS spectrum of bulk In_2O_3 to the total signal obtained for the catalyst to obtain the EXAFS spectrum of the I_3 site. Figure 5 shows the Fourier transform of the difference spectrum obtained subtracting the In_2O_3 spectrum weighted with the percentage (54%) of the oxide in the catalysts—determined by PAC—to the In/ZSM 5 EXAFS spectrum. The inset shows the backtransform of the peak in the range 0.9-2.6 Å and the fitted EXAFS functions obtained using phase and amplitudes generated by the FEFF code [21]. The parameters obtained are shown in Table II. Two oxygen shells and one aluminum shell were found in the fitting procedure. One oxygen atom is located at 2.10 Å while 2 oxygen atoms are at 2.20 Å. These last two oxygen atoms would belong to the zeolite structure and would be bound to an aluminum atom forming an acid site. The distance of the aluminum atom to the In atom is 2.59 Å. The closer oxygen atom is forming the $(\text{InO})^+$ species proposed as the active site and the shorter distance is consistent with a double bond. It is seen that the Debye-Waller factor of the second and third shells are large. This behavior can be understood because of the different configurations in which the $(\text{InO})^+$ species can be bound to different acid sites of the zeolite, leading to slightly different distances In-O (2nd shell) and In-Al. Similar values have been found for small Pt clusters inside zeolite channels [22]. Using theoretical calculations, Jentys et al. found that Pt particles inside zeolite channels have Debye-Waller factors two orders of magnitude larger than an isolated Pt particle. They assigned this effect to an exponential damping of the EXAFS signal resulting from contributions of the zeolite lattice atoms. The several anchoring configurations of the $(\text{InO})^+$ species would also explain the high EFG distribution of I_3 found by PAC (see Table I). Because of the size of the monometallic species, the active site can only be found in the 10-atom ring (8

Å diam.) of the ZSM 5 zeolite as it would not fit in the 6-atom ring (5 Å diam.).

Consequently, by means of XAFS, TDPAC and SAXS experiments we determined the local structure of extremely nanosized In-O species (with the geometry indicated in Table II), responsible for the SCR of NO_x , located inside the larger ZSM 5 zeolite channel.

We wish to dedicate this article to our colleague and friend Patricia Massob in the 10th anniversary of her early death. This research was partially supported by ANPCyT, CONICET, and Fundacion Antorchas (Argentina), by LURE (CNRS, France), and LNLS (Brasil) under project SAXS 314/97. Authors express gratitude to I. Torriani for her assistance at the SAXS beam line.

-
- [1] J. Liet al, Science 299, 864 (2003); Y. Nishihata et al, Nature 418, 164 (2002); M. Valden, X. Lai, and D.W. Goodman, Science 281, 1647 (1998).
 - [2] R.B. Gregor, N.E. Pingitore Jr., and F.W. Lytle, Science 275, 1452 (1997).
 - [3] D. Bazin, Top. Catal. 18, 79 (2002).
 - [4] W. Li, G.D. Meitzner, R.W. Borry III and E. Iglesia, J. Catal. 191, 373 (2000); V. Schwartz, S.T. Oyama, and J.G. Chen, J. Phys. Chem. B 104, 8800 (2000).
 - [5] B.K. Teo, EXAFS: Basic Principles and Data Analysis (Springer-Verlag, Munich, 1986).
 - [6] F.M.F. de Groot, Topics in Cat. 10, 179 (2000).
 - [7] A. Lerf and T. Butz, Angew. Chem. Int. Ed. Engl. 26, 110 (1987); J. Meerschaert et al, Phys. Rev. Lett. 75, 1638 (1995); M. Dippel et al, Phys. Rev. Lett. 87, 95505 (2001); K. Potzger et al, Phys. Rev. Lett. 88, 247201 (2002).
 - [8] S. Lany et al, Phys. Rev. B 62, R2259 (2000); L.A. Erriico et al, Phys. Rev. Lett. 89, 55503 (2002); A.T. Motta et al, Phys. Rev. B 65, 14115 (2001); L.A. Terrazos et al, Solid State Commun. 121, 525 (2002).
 - [9] M. Ogura, M. Hayashi, and E. Kkuchi, Catal. Today 42, 159 (1998).
 - [10] E.E. Miro et al, J. Catal. 188, 375 (1999).
 - [11] E. Kkuchi et al, J. Catal. 161, 465 (1996); X. Zhou et al, J. Mol. Cat. A: Chem. 122, 125 (1997); M. Ogura et al, Cat. Today 42, 159 (1998).
 - [12] C. Schmidt et al, J. Phys. Chem. B 106, 4085 (2002).
 - [13] H. Frauenfelder and R. Steen, in -, -, and -Ray Spectroscopy, edited by K. Siegbahn (North-Holland, Amsterdam), Vol. 2, 917 (1968).
 - [14] S. Habenicht et al, Z. Phys. B 101, 196 (1996).
 - [15] A.G. Biliboni et al, Phys. Rev. B 29, 1109 (1984).
 - [16] T. Ressler et al, J. Phys. Chem. B 103, 6407 (1999).
 - [17] G. Kellem et al, J. Appl. Crystallogr. 30, 880 (1997).
 - [18] O. Glatte and O. Klatky, Small Angle X-Ray Scattering (Academic, London, 1982).
 - [19] A.V. Semenyuk and D.I. Svergun, J. Appl. Crystallogr. 24, 537 (1991).
 - [20] A. Benedetti, J. Appl. Cryst. 30, 647 (1997).
 - [21] S.I. Zabinsky et al, Phys. Rev. B 52, 2995 (1995).
 - [22] A. Jentys, L. Simon, and J.A. Lercher, J. Phys. Chem. B 104, 9411 (2000).